MDPI

Article

Experimental Investigations of Expansion Strength of Hydraulic Expansion Joints Interconnecting Tube and Fins Heat Exchanger

Haimei Han, Lianfa Yang *, Jingyu Jiang and Jianping Ma

School of Mechanical and Electrical Engineering, Guilin University of Electronic Technology, Guilin 541005, China; hanhaimei@guet.edu.cn (H.H.); j_jingyu@163.com (J.J.); majianping1229@163.com (J.M.)

* Correspondence: y-lianfa@163.com

Abstract: As a high expansion strength corresponds to a high heat transfer efficiency, this study investigated the expansion strength of an air-conditioning heat exchanger jointed by hydraulic expansion. A device that would be reliable and adaptable to different types of tubes and fins was designed and developed for testing hydraulic expansion. The device was used to perform a non-pulsating hydraulic expansion experiment on samples comprising tubes and fins to determine the hydraulic pressure range. The expansion strength was tested by performing tensile tests to evaluate the pull-out force at different bulging zones of the same sample with the selected hydraulic pressure. A series of pulsating hydraulic expansion experiments were performed on the joints of tubes and fins with different pulsating amplitudes and frequencies. Tensile tests were performed on the pulsating hydraulic expansion samples to study the influence of the pulsation parameters on the pull-out force. When the amplitude was fixed, an increase in frequency led to uniform expansion in the exchanger. This indicates that joint expansion in tubes and fins results in a more reliable heat exchanger performance.

Keywords: heat exchanger; hydraulic expansion; pulsation parameter; bulging zone; pull-out force

1. Introduction

The air heat exchanger is the core component of an air-conditioning system because heat exchange occurs in it. An air heat exchanger comprises copper tubes with a spiral-grooved inner surface and hydrophilic aluminium foil fins. The grooved inner surface of the tubes, collar design, and uneven structures on both sides of the fin increase the heat transfer efficiency by 20–30% and reduce energy consumption by 15% compared to a smooth inner structure [1–3]. This heat exchanger design is widely applied in power generation, air conditioning, and many other industries. Energy-saving air conditioners are suitable for applications requiring reductions in energy consumption and emissions [4]. Figure 1 shows an air heat exchanger.
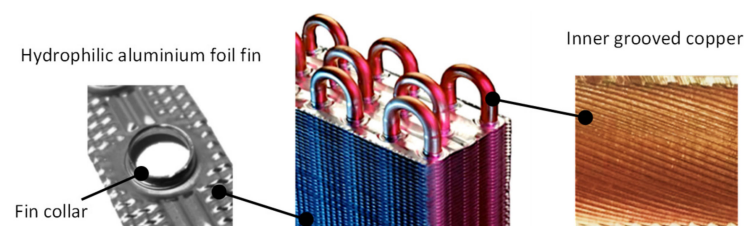

Figure 1. Air heat exchanger, comprising inner grooved copper tubes and hydrophilic aluminium foil fins.

A heat exchanger can be designed with small-diameter heat exchange tubes and fins, which help maintain the heat transfer performance and reduce the weight, package volume, airflow resistance, and manufacturing complexity [5]. Although reducing the tube diameter decreases the heat exchange area, it improves the heat transfer performance. For example, using a Φ5 mm tube instead of a Φ9.52 mm tube increases the heat transfer coefficient by 10%. In addition, the reduced amount of copper reduces the cost by more than 50% and the filling volume by about 25% [6]. Therefore, research on the joints of small-diameter heat exchange tubes and fins is of great significance.

To improve the joints of tubes and fins, tube hydroforming (THF) is an alternative to mechanical roll expansion that uses hydraulic fluid as a uniform forming medium to transform metal tubes into complex hollow parts [7]. THF can be applied to heat exchange tubes and fins to solve problems such as the wrinkles and bending caused by mechanical roll expansion. THF does not damage the inner grooved structure. Typically, THF results in a 1–3% wall reduction due to the uniform hydraulic pressure; in contrast, mechanical roll expansion results in a reduction of 3–12% because of the uneven axial compression [8]. Consequently, THF can potentially be applied to the joints of heat exchangers, which undergo an expansion process, as shown in Figure 2. However, research on the hydraulic expansion of tubes has been limited.
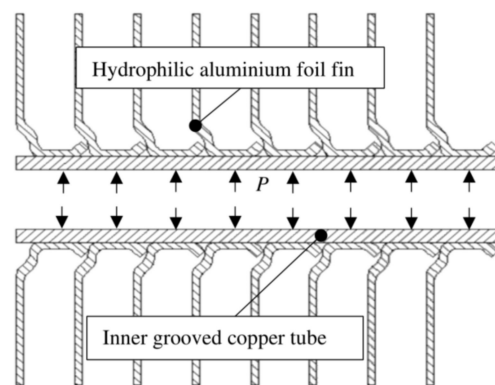

Figure 2. Diagram of the hydraulic expansion process in the air heat exchanger.

Tube hammering/pulsating hydroforming was first proposed by Rikimaru and Ito [9] in 2001 and was applied to the hydraulic expansion of a tube to improve performance. They found that applying pulsating hydroforming could delay the rupture time of tubes [9]. In 2004, Di Lorenzo et al. [10] used artificial intelligence techniques, numerical simulations, and experiments to realize a tube hydroforming design. Other research on tube hammering/pulsating hydroforming has shown that hydraulic expansion increases the height of the expanded tube and produces a more uniform wall thickness in the bulging zone of the tube [11,12]. Yang et al. [13] and Mohamed et al. [14] simulated the pulsating hydroforming process while considering the expansion pressure and time increment. They proposed new indicators for evaluating the uniformity of the tube wall thickness, reliability, moulds fillability. They found that the expansion of the tube increased as the expansion pressure and time increment decreased and the pulsating hydraulic amplitude increased. Thus, tube hammering/pulsating hydroforming is considered a promising method for fabricating the joints of heat exchange tubes and fins and improving the reliability of heat exchangers.

An important mechanical property [15] for the performance of the heat exchanger is the expansion strength [16] of the joint between a tube and fin, which is denoted by the pull-out force. The pull-out force after hydraulic expansion is mostly evaluated through tensile tests. Merah et al. [17,18] performed finite element analysis and found that, for low clearances, the calculated residual contact pressure of the analytical results compares well with those inferred from the experimentally measured pull-out force. Wang et al. [19] used the finite element method to analyse a shell-and-tube multiple fixed-tube plate heat

exchanger for three cases and calculated the pull-out force for a heat exchanger and tube-sheets at different temperature distributions. Their results showed that the effect of the pull-out force on the different locations of a heat exchanger tube is greater for multiple exchangers. However, most of the above studies were based on mechanical roll expansion. Few studies have evaluated the pull-out force of tubes and fins in air heat exchangers fabricated by hydraulic expansion.

In this study, a device was designed for the hydraulic expansion of heat exchange tubes and fins; the device is reliable and adaptable to tubes and fins of different numbers and lengths. A non-pulsating hydraulic expansion experiment was performed on test samples comprising copper tubes and fins. Based on the experimental results, the appropriate hydraulic pressure range was determined. The same test results were used to evaluate the pull-out force of different bulging zones of the same test sample expanded at the proper hydraulic pressure. The influence of different bulging zones on the pull-out force of heat transfer tubes was evaluated. A hammering/pulsating hydraulic expansion test was applied to the joints of tubes and fins with a varying pulsating amplitudes and frequencies. After the expansion, a tensile test was performed on the samples, and the maximum pull-out force with different pulsation parameters was determined. The results were used to characterise the influence of the pulsation parameters on the pull-out force.

2. Geometries of Tubes and Fins

The study objects were seamless inner grooved copper tubes and hydrophilic aluminium foil fins. Figure 3 shows the heat exchange tubes and fins that formed the test sample, and Table 1 lists their geometric and material properties. The seamless inner grooved tubes were composed of TP2 copper, and the hydrophilic aluminium foil fins were composed of 8006 aluminium. The dimensions are also shown in Figure 3.
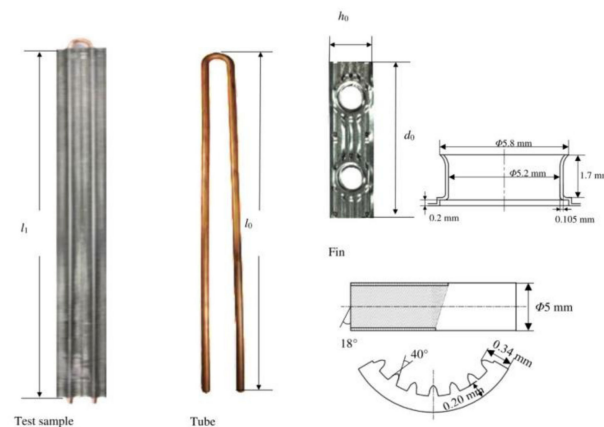

Figure 3. Test sample comprising details of cross-section of tubes and fins.

Table 1. Geometric and material parameters of the TP2 tube and fin made of 8006 aluminium.

Tube	Value	Fin	Value
Outer diameter Φ_0 (mm)	5	Arrangement length l_1 (mm)	355
Wall thickness δ (mm)	0.5	Width d_0 (mm)	40
Length l_0 (mm)	375	Height h_0 (mm)	11
Density (g·cm^{-3})	8.916	Density (g·cm^{-3})	2.780
Young's modulus (GPa)	127	Young's modulus (GPa)	68
Poisson's ratio	0.33	Poisson's ratio	0.33
Tensile stress (MPa)	205.807	Tensile stress (MPa)	136.889
Yield stress (MPa)	66	Yield stress (MPa)	132

3. Design of the Hydraulic Expansion Device

The joints of air heat exchangers are mostly formed by mechanical roll expansion; hydraulic expansion has not been promoted. Therefore, mature equipment for expanding

the test samples was not available, especially those with small diameters. One of the primary contributions of this study was the design and development of a hydraulic expansion device suitable for small-diameter heat exchange tubes and fins.

The self-designed hydraulic expansion device comprises a hydraulic pressure generator, liquid sealing system, and the test sample location. Designing each component required considering the sealing performance during the expansion process. In addition, the applicability and flexibility of the device needed to be considered.

(1) Hydraulic pressure generator: This is a liquid-filled bolt connected to an external pressure liquid supply system. The liquid-filled bolt has a through-hole in the middle. One end of the bolt is connected to the liquid supply apparatus, and the other end is connected to the heat exchange tube.

(2) Liquid sealing system: Each end of the tube is connected to a fastening tube sleeve and sealing nut. The tube sleeve has two threaded holes to connect the sealing nut and liquid-filled bolt. To ensure the sealing performance, both ends of the tube are connected with the liquid-filled bolt, and the sealing nut has an O-ring to prevent liquid leakage when the device is hydraulically expanded. The O-rings act together with the threaded hole in the tube sleeve to form a tightening seal with the sealing nut and liquid-filled bolt.

(3) Test sample location: This part comprises two long screws, a fastening tube sleeve, and a guiding sleeve. Both sleeves have through-holes to allow the long screw to pass through, and the nut is tightened to support the device. A flexible cushion block is between the guiding sleeve and end of the tube to protect the tube during hydraulic expansion. To ensure the applicability and flexibility of the device, the guiding sleeve and fastening sleeve were designed with the same external dimensions and volume. The two ends of the sleeves have through-holes for the long screw to pass through to cooperate with the nut. Hence, the device can adapt to different lengths of tubes and numbers of fins.

Figure 4 shows the structure and photographs of the test sample and device. The assembly process was as follows. First, the fins were placed on the tube and pressed against each other to eliminate any gaps. The two ends of the tube were inserted in the holes of the fastening sleeve. Second, the O-rings were placed on the two ends of the tube, and the short end of the liquid-filled bolt was placed at one end and screwed in to form a seal. Third, the long end of the liquid-filled bolt was connected to the liquid supply device, which was operated until liquid flowed from the other end of the tube to ensure that any remaining air was removed. Fourth, the sealing nut was screwed into the other end of the tube to form a seal. Finally, the threaded end of the long screw was inserted into the through-holes on both sides of the fastening sleeve and the guiding sleeve and screwed in with a nut.
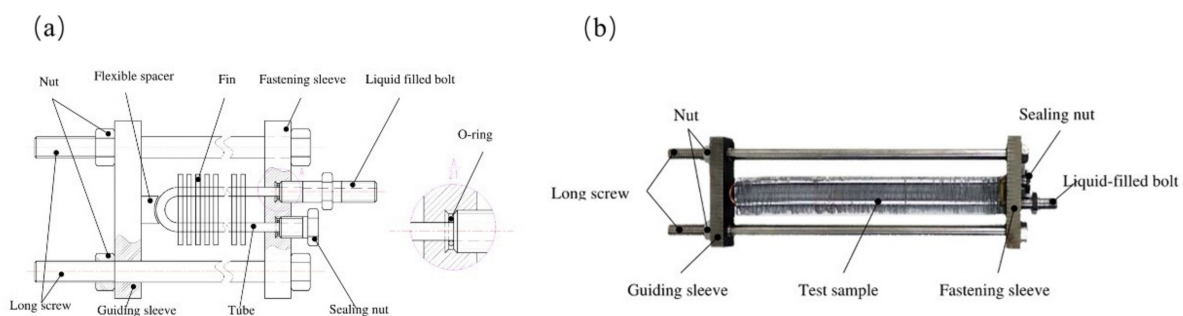

Figure 4. The hydraulic expansion device and sealing part. (**a**) The design of the device; (**b**) The photo of device.

4. Experiments

4.1. Non-Pulsating Hydraulic Expansion

Non-pulsating hydraulic expansion was performed for a preliminary observation of the joint of the test sample. Eight to ten tests were conducted on each sample under the same experimental conditions, and three to five similar results were selected as our experimental data. Accordingly, the proper expansion pressure range of the small-diameter tube and fins was determined for the pulsating hydraulic expansion and tensile tests. Figure 5a–e show the parts of the experimental platform.
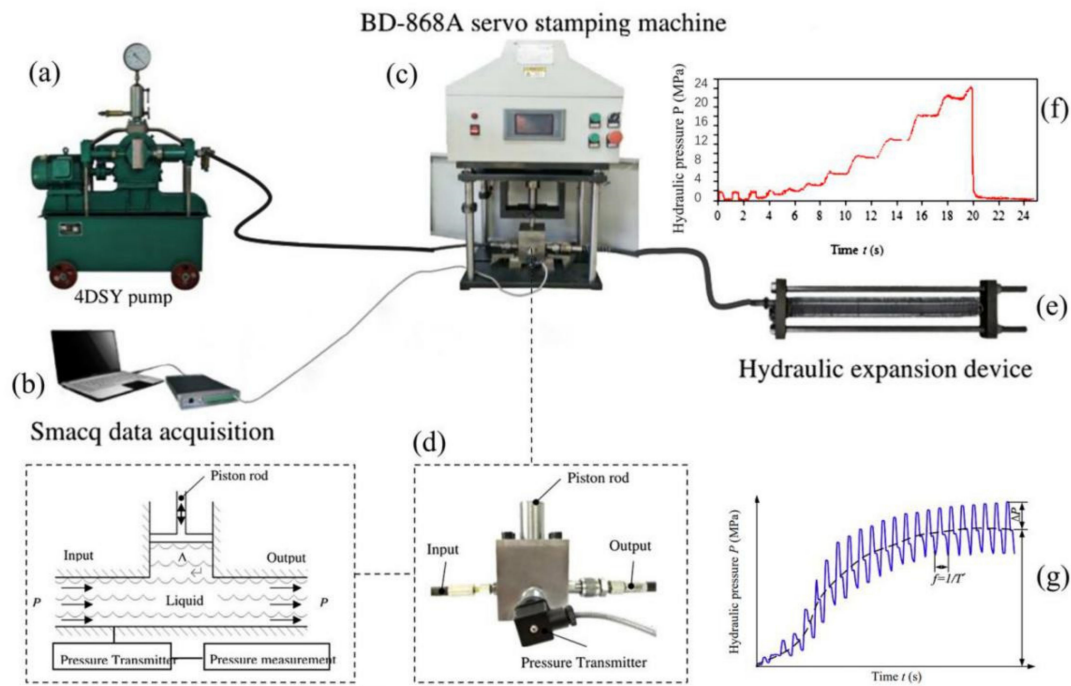

Figure 5. Non-pulsating and pulsating hydraulic expansion experimental platform. (**a**,**d**) External pressure liquid supply device; (**b**) data acquisition system; (**c**) stamping machine; (**e**) self-designed hydraulic expansion device; (**f**) non-pulsating hydraulic pressure; (**g**) pulsating hydraulic pressure.

A pump was utilised as the external pressure liquid supply device and could supply a continuously rising pressure. After the expansion device and test sample were assembled, the air inside the tube was evacuated, and the tightness of the device was checked. The pump was connected to supply hydraulic pressure, and the expansion process was observed for further analysis. Smacq multifunctional data acquisition equipment is well designed to meet various testing needs. Figure 5f shows the acquired curve of the hydraulic pressure with the loading time. The fluctuations in the curve indicate natural fluctuations of the liquid, which differ from that due to pulsating hydraulic expansion.

The first hydraulic expansion experiment showed that the test sample may bend as the tube decreased in diameter and increased in length and as the loading speed of the liquid increased. Figure 6a shows a bent test sample. When the liquid leaked upon the sample bending, the maximum pressure was only 11 MPa. Thus, the tube and fins were not jointed well. Reducing the hydraulic pressure loading speed of the 4DSY pump (i.e., pressure frequency of the liquid) during the test prevented the copper tube from bending and improved the forming quality. In subsequent tests, the hydraulic pressure loading speed of the 4DSY pump was reduced; the tube did not bend, and the liquid did not leak out. After many non-pulsating hydraulic expansion tests, the test samples began to expand outward at a hydraulic pressure of about 10 MPa, and the samples burst at a maximum hydraulic pressure of about 24 MPa. Figure 6b shows a burst sample.

Figure 6. (**a**) Bending failure and (**b**) bursting failure in the sample due to hydraulic expansion.

To evaluate the proper expansion pressure for hydraulic expansion of the air heat exchanger, maximum pressures of 14, 16, 18, and 20 MPa were considered. After the hydraulic pressure reached the pre-set value, the hydraulic expansion device was disassembled. Then, the test sample was taken out of the self-designed device after expansion. This completed the non-pulsating hydraulic expansion experiment.

4.2. Pulsating Hydraulic Expansion

To evaluate the influence of pulsating hydraulic parameters on the pull-out force, multiple tensile tests were conducted on multiple sets of pulsating hydraulic expansion experiments with varying amplitudes and frequencies. To study the effect of the pulsating hydraulic parameters on the pull-out force, the maximum pressure for pulsating hydraulic expansion needed to be established within the range set for non-pulsating hydraulic expansion. In addition to the apparatus of the non-pulsating hydraulic expansion experiment, the BD-868A servo stamping machine shown in Figure 5c was used in the pulsating hydraulic expansion experiments. Figure 5a–e show parts of the experimental platform for pulsating hydraulic expansion [20].

The BD-868A servo stamping machine could move the mould up or down under manual or automatic control. The hydraulic pressure was output through the 4DSY pump and flowed through the pulsating hydraulic pressure generator. The piston rod of the device could generate a given amplitude and frequency based on the reciprocating motion of the screw in the BD-868A servo stamping machine. The parameters could be varied by adjusting the stamping stroke and motor speed of the servo stamping machine. Figure 5 shows the pulsating hydraulic pressure generator and its working principle. The stroke s of the servo stamping machine affected the pressure amplitude ΔP, and the motor speed n affected the pulsation frequency f. Table 2 presents the parameter settings of the servo stamping machine during the pulsating hydraulic expansion test and the calculated pulsation parameters.

Table 2. Settings for the stroke and speed of servo stamping machine and the pulsation parameters of the amplitude and frequency.

Stroke s (mm)	Speed n (r/min)	Amplitude ΔP (MPa)	Frequency f (c/s)
2	200	1.72	0.67
4	500	2.83	1.29
6	800	3.53	1.8

The difference between the pulsating and non-pulsating hydraulic experiments was how hydraulic pressure was applied. If the loading curve of the non-pulsating hydraulic expansion is taken as the reference, then the pulsating hydraulic pressure was applied by adjusting the amplitude and frequency. Figure 5g shows a representative curve of the pulsating hydraulic expansion varying with the loading time. Applying a pulsation amplitude to a non-pulsating hydraulic expansion pressure of 18 MPa may cause over-expansion of the tube, so a median value of 17 MPa was selected to ensure that the test pressures remained within the proper hydraulic pressure range.

The process of the pulsating hydraulic expansion experiment was as follows. Before the pulsation experiment, the tube and fins were punctured and fixed to the self-designed

hydraulic device. The air in the tube was evacuated, and special care was taken with ensureing the airtightness of the device. Then, the 4DSY pump was connected with the pulsating hydraulic pressure generator, data acquisition system, and self-designed hydraulic expansion device. The pulsating hydraulic pressure generator was fixed under the servo stamping machine. As given in Table 2, the stroke was set to 2 mm, and the motor speed was set to 200 r/min. The stamping stroke was set to be the same as the first return stroke. Thus, the stop time was set to 0, and the number of times was set to a higher value. Next, the servo stamping machine and data acquisition card were started, and the 4DSY pump was operated to output a continuously increasing hydraulic pressure. The screw of the servo stamping machine drove the piston rod to move up and down as it pressed the liquid in the hydraulic chamber. The maximum hydraulic pressure value was controlled at about 17 MPa. Finally, the measurement data were recorded in a computer and output into figures and tables for later data analysis and calculation of the amplitude and frequency.

When the stamping stroke s was 2 mm and the motor speed n was 200 r/min, the pulsation parameter amplitude ΔP was 1.72 MPa and the frequency f was 0.67 c/s. Thus, the amplitude and frequency were calculated according to the other parameters. Table 3 gives the nine groups of data combinations used to obtain different amplitudes and frequencies. Each group of experiments was carried out three times to eliminate accidents and improve accuracy.

Table 3. Pulsation parameters of the amplitude and frequency in the experiment.

Stroke s (mm)	Speed n (r/min)	Amplitude ΔP (MPa)	Frequency f (c/s)
2	200	1.72	0.67
2	500	1.72	1.29
2	800	1.72	1.80
4	200	2.83	0.67
4	500	2.83	1.29
4	800	2.83	1.80
6	200	3.53	0.67
6	500	3.53	1.29
6	800	3.53	1.80

4.3. Tensile Tests

The pull-out force was obtained from tensile tests carried out after the non-pulsating and pulsating hydraulic expansion experiments. The test sample after the hydraulic expansion experiment was cut into pieces of tube and fins with a handheld cutting machine. Figure 7 shows the tensile test platform, which comprised a material testing machine, data acquisition system, and tensile test device. The tensile test samples were fixed in the tensile test device, which was connected with the material testing machine. The tensile test samples were made from the non-pulsating hydraulic expansion samples at the proper expansion pressure, and each expansion sample was cut into four parts labelled A, B, C, and D [21]. The samples were cut into four parts because stress concentrations were generated at bends of the tube, and the number of fins on the left end of the sample was not sufficient for an entire sample. Figure 8 shows that each part was cut into two smaller samples labelled 1 and 2 to increase the number of test samples. The dashed line denotes the cutting location. The beam of the material testing machine was stretched upward at a uniform speed of 5 mm/s to pull the fins off the tube. The tensile tests were used to evaluate the influence of the non-pulsating hydraulic expansion pressure on the pull-out force and determine the proper expansion pressure value.
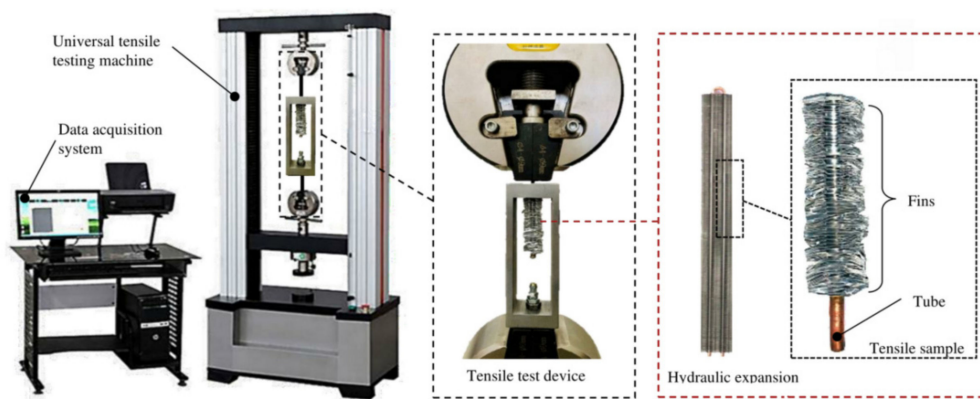
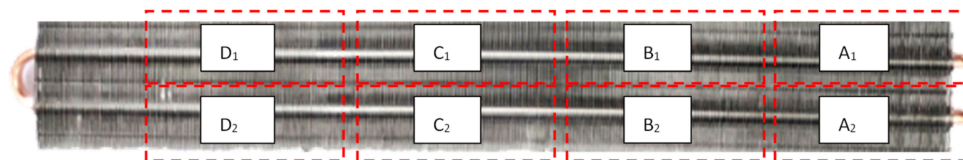**Figure 7.** Tensile test platform.

Figure 8. Eight samples in the tensile test cut along the dashed lines.

For the tensile test of the pulsating hydraulic expansion samples, most of the experimental steps were the same as those for the non-pulsating hydraulic expansion samples. However, the nine sets of test samples given in Table 3 were tested to facilitate the collection and recording of experimental data. The curve of the time and strength was observed and recorded in real time, which was convenient for calculation and analysis.

5. Results and Discussion

5.1. Proper Hydraulic Pressure Range

In the non-pulsating hydraulic expansion experiment, the tube and fins expanded at 14 MPa were not jointed tightly, and the fins easily slipped down the tube, as shown in Figure 9a. However, the tube and fins were over-expanded at 20 MPa, as shown in Figure 9b. The samples were expanded tightly at 16 to 18 MPa, and the tubes and fins were jointed well without overexpansion. The non-pulsating hydraulic expansion experiment showed that the self-designed hydraulic expansion device can meet the requirements for hydraulic expansion, and the proper hydraulic expansion pressure for the test samples was determined to be 16–18 MPa. To determine the proper hydraulic expansion pressure more accurately for the tensile test, test samples were jointed at 16, 17, and 18 MPa three times at each pressure.
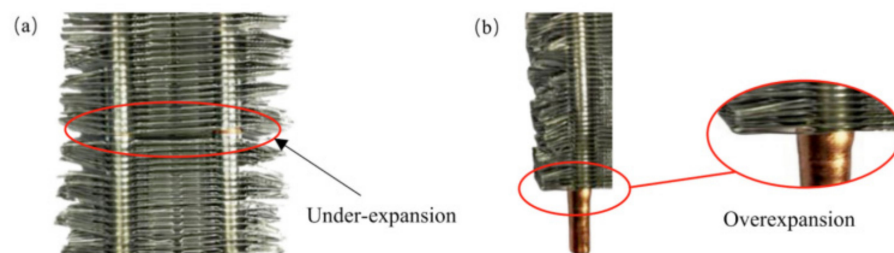

Figure 9. Sample jointed at a hydraulic pressure of (**a**) 14 MPa and (**b**) 20 MPa.

Tensile tests were performed on samples formed at the maximum hydraulic pressures (P_{max}) of 16, 17, and 18 MPa and cut from hydraulic expansion samples (e.g., 1a/1b,

2a/2b, 3a/3b, and 4a/4b) with the material testing machine. The tube of each sample was pulled, and the pull-out force was recorded with the data acquisition system. The values for the maximum pull-out force (F_{max}) of the tensile test samples at 16, 17, and 18 MPa were averaged, as given in Table 4. The results showed that the samples could withstand F_{max} = 0.47 kN at P_{max} = 18 MPa. Thus, the proper hydraulic expansion pressure was determined to be 18 MPa.

Table 4. Average value of F_{max} of tensile test samples at P_{max} of 16, 17, and 18 MPa.

P_{max} (MPa)	F_{max} (kN)
16	0.36
17	0.38
18	0.47

5.2. Pull-Out Forces in the Bulging Zones

Figure 10 shows the fitting of the data obtained from the tensile test of the samples formed by non-pulsating hydraulic expansion at 16, 17, and 18 MPa. The results indicate that the samples could withstand F_{max} at P_{max} = 18 MPa. Thus, the proper hydraulic expansion pressure was determined to be 18 MPa. For all samples, section C could withstand a larger pull-out force than the other sections [22]. The maximum pull-out force (F_{max}) of each section of the test sample is summarised in Table 5 and visualised in Figure 11. The results showed that the middle section of the samples could withstand a greater pull-out force than the other sections, indicating that the middle section also provided more reliable results.
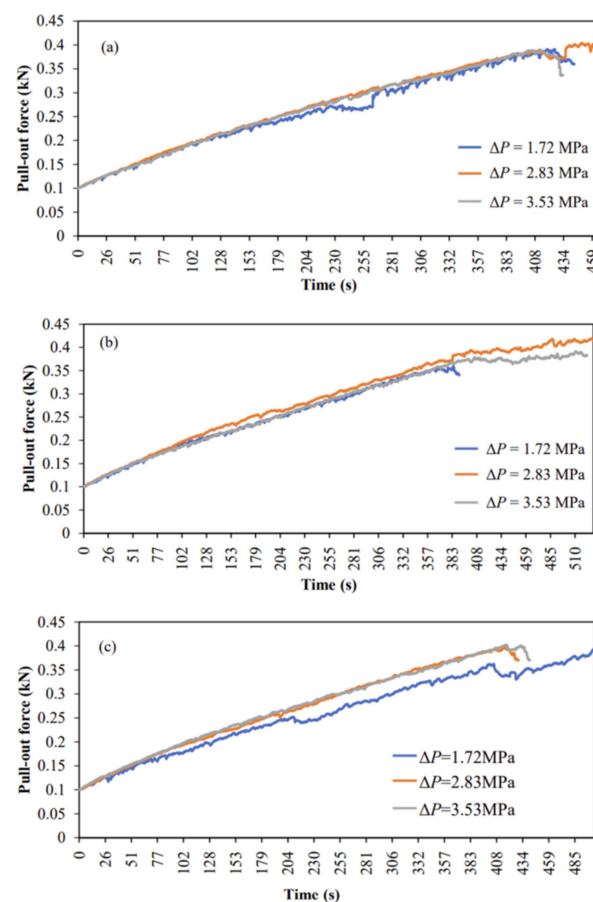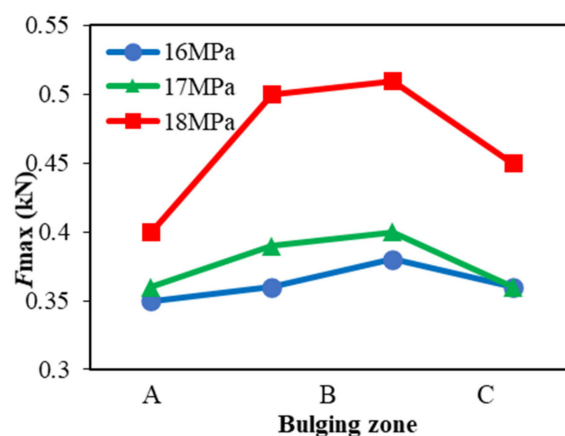

Figure 10. Variation in the pull-out force with the loading time at different hydraulic expansion pressures: (**a**) 16, (**b**) 17, and (**c**) 18 MPa.

Table 5. F_{max} that each part of the test sample could withstand at P_{max} = 16, 17, and 18 MPa.

P_{max} (MPa)	F_{max} (kN)			
	A	B	C	D
16	0.35	0.36	0.38	0.36
17	0.36	0.39	0.40	0.36
18	0.40	0.50	0.51	0.45

Figure 11. Variation in F_{max} at different bulging zones of tensile test samples and 16, 17, and 18 MPa.

5.3. Effect of Pulsation Parameters on the Pull-Out Force

Table 6 summarises the groups of pulsation parameters and corresponding F_{max} after the pulsating hydraulic expansion experiment and tensile test. F_{max} was 0.38 kN with non-pulsating hydraulic expansion at 17 MPa. In contrast, F_{max} was 0.42 kN with pulsating hydraulic expansion and the different groups of pulsation parameters. Hence, pulsating hydraulic expansion can improve the expansion performance of tubes and fins.

Table 6. F_{max} corresponding to each group of ΔP and f.

ΔP (MPa)	f (c/s)	F_{max} (kN)
1.72	0.67	0.391
1.72	1.29	0.394
1.72	1.80	0.359
2.83	0.67	0.404
2.83	1.29	0.396
2.83	1.80	0.419
3.53	0.67	0.389
3.53	1.29	0.403
3.53	1.80	0.391

5.3.1. Pulsation Amplitude

Figure 12 shows the relationship between the amplitude and maximum pull-out force. When $\Delta P \leq 2.83$ MPa, the pull-out force increased with the amplitude; however, the pull-out force decreased with increasing amplitude when $\Delta P > 2.83$ MPa. When $\Delta P = 2.83$ MPa, the maximum pull-out force peaked at 0.406 kN.
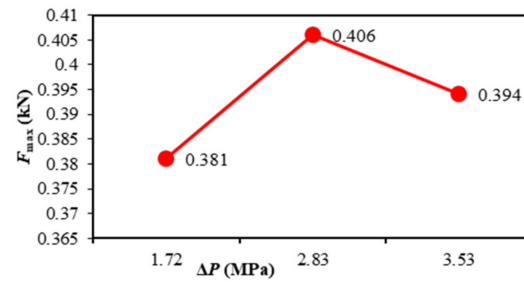
Figure 12. Variation in F_{max} with ΔP at the same frequency.

5.3.2. Pulsation Frequency

Tensile tests were performed on pulsating hydraulic expansion samples subjected to the same amplitude and different frequencies [23]. At frequencies of 0.67, 1.29, and 1.80 c/s, the curve of the pull-out force varied with time for the three amplitudes, as shown in Figure 13. Increasing the pulsation frequency caused the curve of the pull-out force to change more smoothly and rise steadily with little fluctuation. When the amplitude was fixed, increasing the frequency increased the uniformity of the joint between the tube and fin, which increased the reliability.
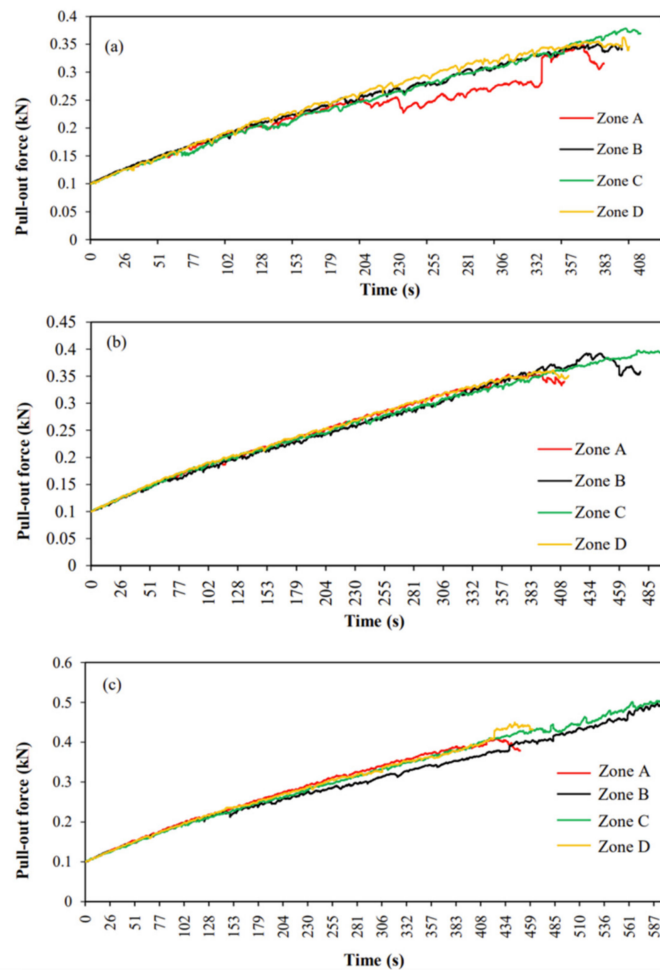

Figure 13. Variation in the pull-out force over time for the three amplitudes and three frequencies: (**a**) 0.67, (**b**) 1.29, and (**c**) 1.80 c/s.

6. Conclusions

A self-designed hydraulic expansion device was used to perform experiments on non-pulsating and pulsating hydraulic expansion. In addition, tensile tests were performed to investigate the pull-out force of heat exchange tubes and fins after hydraulic expansion. The following conclusions were drawn:

(1) In the proper hydraulic expansion range of 16–18 MPa, $F_{\max}$ was 0.47 kN at a $P_{\max}$ of 18 MPa. Thus, the proper hydraulic expansion pressure of the test samples was determined to be 18 MPa.

(2) The middle section of the test sample could withstand a higher pull-out force than the other sections, which provided better reliability in the hydraulic expansion tests.

(3) When $\Delta P \leq 2.83$ MPa, the pull-out force increased with the amplitude; when $\Delta P > 2.83$ MPa, the pull-out force decreased with increasing amplitude. At $\Delta P = 2.83$ MPa, the maximum pull-out force peaked at 0.406 kN.

(4) When the amplitude was fixed, increasing the frequency increased the uniformity of the joint between the tube and fin, which improved the reliability of the joint.

Author Contributions: Conceptualization, H.H. and L.Y.; Data curation, H.H. and J.M.; Formal analysis, H.H. and J.J.; Funding acquisition, L.Y.; Investigation, H.H., J.J. and J.M.; Methodology, H.H.; Project administration, L.Y.; Resources, H.H., L.Y. and J.J.; Supervision, L.Y.; Validation, H.H., J.J. and J.M.; Writing—original draft, H.H.; Writing—review & editing, H.H. and L.Y. All authors have read and agreed to the published version of the manuscript.

Institutional Review Board Statement: Not applicable.

Informed Consent Statement: Not applicable.

Data Availability Statement: Not applicable.

Conflicts of Interest: The authors declare no conflict of interest.

References

1. Kaji, R.; Yoshioka, S.; Fujino, H. The Effect of Inner Grooved Tubes on the Heat Transfer Performance of Air-cooled Heat Exchangers of CO_2 Heat Pump System. In Proceedings of the International Refrigeration and Air Conditioning Conference, Purdue University, West Lafayette, IN, USA, 16–19 July 2012.
2. Al-Shamani, A.N.; Sopian, K.; Mohammed, H.A.; Mat, S.; Ruslan, M.H.; Abed, A.M. Enhancement Heat Transfer Characteristics in the Channel with Trapezoidal Rib-groove Using Nanofluids. *Case Stud. Therm. Eng.* **2015**, *5*, 48–58. [CrossRef]
3. Rahman, M.M.; Zhen, T.; Kadir, A.K. Numerical Simulation of Fluid Flow and Heat Transfer in Enhanced Copper Tube. In Proceedings of the IOP Conference Series: Earth and Environmental, Putrajaya, Malaysia, 5–6 March 2013.
4. Maneewan, S.; Tipsaenprom, W.; Lertsatitthanakorn, C. Thermal Comfort Study of a Compact Thermoelectric Air Conditioner. *J. Electron. Mater.* **2010**, *39*, 1659–1664. [CrossRef]
5. Cox, T.L.; Patel, R.L. Small Diameter in Line Tube and Fin Aluminum Heat Exchanger for Automotive Air Conditioning Sys-tems. In Proceedings of the Sae International Congress & Exposition, Warrendale, PA, USA, 27 February 1989.
6. Ding, G.; Wu, G.; Liu, T. Development of Heat Exchanger for Refrigeration and Air-Conditioning–Fin-and-tube Heat Ex-changers Using Small Diameter Tubes. *J. Appl. Sci. Technol.* **2019**, *4*, 40–45.
7. Yang, L.; Zhao, Q. Forming Limit Diagrams for Tubes with Non-uniform Thickness in Hydro-bulging. *Int. J. Adv. Manuf. Technol.* **2019**, *103*, 901–911. [CrossRef]
8. Yokell, S. Expanded, and Welded-and-Expanded Tube-to-Tubesheet Joints. *J. Press. Vessel Technol.* **1992**, *114*, 157–165. [CrossRef]
9. Rikimaru, T.; Ito, M. Hammering Hydroforming of Tubes. *Press Work.* **2001**, *39*, 58–65.
10. di Lorenzo, R.; Filice, L.; Umbrello, D.; Micari, F.; Ghosh, S.; Castro, J.C.; Lee, J.K. An Integrated Approach to the Design of Tube Hydroforming Processes: Artificial Intelligence, Numerical Analysis and Experimental Investigation. *AIP Conf. Proc.* **2004**, *712*, 1118–1123.
11. Khalili, K.; Ahmadi-Brooghani, S.Y.; Ashrafi, A. Investigation on the Effect of Pulsating Pressure on Tube-Hydroforming Process. *Key Eng. Mater.* **2011**, *473*, 618–623. [CrossRef]
12. Loh-Mousavi, M.; Mirhosseini, A.M.; Amirian, G. Investigation of Modified Bi-Layered Tube Hydroforming by Pulsating Pressure. *Key Eng. Mater.* **2011**, *486*, 5–8. [CrossRef]

13. Yang, L.F.; Chen, F.J. Investigation on the Formability of a Tube in Pulsating Hydroforming. *Mater. Sci. Forum* **2009**, *628–629*, 617–622. [CrossRef]

14. Mohamed, M.; El-Aty, A.A.; Abdel Aziz, H.; Nader, F. Theoretical Investigations and Simulation of the Hydroforming Processes Performed on c1010 Low Carbon Steel Tubes. *Appl. Mech. Mater.* **2015**, *799–800*, 443–447. [CrossRef]

15. Yang, Y.; Fan, L.; Xu, C.; Dong, X. Experimental Study of Mechanical Properties of 30SiMn2MoVA Steel Gun Barrel Processed by Cold Radial Forging. *ASME J. Press. Vessel Technol.* **2020**, *143*, 011501. [CrossRef]

16. Zheng, M.; Gao, H.; Teng, H.; Hu, J.; TIian, Z.; Zhao, Y. A Simplified Approach for the Hydro-forming Process of Bi-metallic Composite Pipe. *Arch. Metall. Mater.* **2017**, *62*, 879–883. [CrossRef]

17. Merah, N.; Al-Zayer, A.; Shuaib, A.; Arif, A. Finite Element Evaluation of Clearance Effect on Tube-to-tubesheet Joint Strength. *Int. J. Press. Vessel. Pip.* **2003**, *80*, 879–885. [CrossRef]

18. Guan, Y.; Pourboghrat, F.; Barlat, F. Finite Element Modeling of Tube Hydroforming of Polycrystalline Aluminum Alloy Extrusions. *Int. J. Plast.* **2006**, *22*, 2366–2393. [CrossRef]

19. Wang, J.P.; Jin, W.Y.; Wang, X.M.; Gao, Z.L. Study on Pull-out Force in Tube-and-shell Heat Exchangers with Finite Element Method. *Nucl. Power Eng.* **2008**, *29*, 58–61.

20. Ma, J.; Yang, L.; He, Y. Dynamic Frictional Characteristics of TP2 Copper Tubes during Hydroforming under Different Loading and Fluid Velocities. *J. Mater. Eng. Perform.* **2019**, *28*, 3661–3672. [CrossRef]

21. Sadlowska, H.; Morawinsk, L.; Jasinski, C. Strain Measurement in Free Tube Hydroforming Process. *Arch. Metall. Mater.* **2020**, *65*, 257–263.

22. Zhu, H.H.; He, Z.B.; Lin, Y.L.; Zheng, K.L.; Fan, X.B.; Yuan, S.J. The Development of a Novel Forming Limit Diagram under Nonlinear Loading Paths in Tube Hydroforming. *Int. J. Mech. Sci.* **2020**, *172*, 105392. [CrossRef]

23. Guo, T.Y.; Fahrettin, O.; Firas, J.; Jamal, Y.S.A. Analysis of Contact Pressure of Mechanically Lined Corrosion Resistant Alloy Pipe by Hydraulic Expansion Process. *ASME J. Press. Vessel. Technol.* **2017**, *139*, 021212. [CrossRef]